24th COBEM - 2017

24th ABCM International Congress of Mechanical Engineering
December 3-8, 2017, Curitiba, PR, Brazil

COBEM-2017-0241
COMPUTATIONAL FLUID DYNAMICS APPLIED IN A SOLAR CHIMNEY ANALYSIS

Filipe Alcântara Soares
Priscila Pires Araújo
André Luiz Tenório Rezende
Department of Mechanical Engineering, Instituto Militar de Engenharia, RJ, Brazil
alcantara_filipe@hotmail.com, priscila.pires.engenergia@gmail.com, arezende@ime.eb.br

Abstract. *Computational fluid dynamics was used to simulate solar chimney power plants and investigate modeling techniques. The solar chimney combines three known elements: solar air collector, tower and wind turbine. This device uses the solar radiation to generate a hot airflow and this is usually used to drive wind turbines coupled to an electric generator. Large solar chimneys are necessary for be economically competitive with conventional power plants, however small chimneys can be used for other applications, for example drying agricultural products. In order to analyze the turbulent flow in a small solar chimney in this paper, the Finite Volume Method was adopted to solve the system of equations which describe the two-dimensional steady state airflow. The purpose of this work is to verify the influence of the ground in the numerical analysis of airflow in a small solar chimney using three turbulence models: standard k-ε, standard k-ω and the SST k-ω. The simulations are compared with experimental data available in the literature and with another numerical analysis that used the k-ε model. The results showed that the use of the ground as an energy storage layer has not major influence on the temperature and velocity profile of the airflow and for the approach seen in this paper it may be negligible in the numerical analysis.*

Keywords: *Solar chimney, Numerical study, Turbulence models.*

1. INTRODUCTION

Over the time, the energy demand increased in large scale in the world and consequently the use of fossil fuels. Inside this context, environmental impacts caused by them have grown and nowadays concern the society because not only these sources affect the environment but also they are harmful to human health. Another issue is that they are non-renewable resources and are being depleted at high rates. For this reasons, the search for alternative energy sources that are cleaner and cheaper than conventional energies has become extremely important.

Then the solar chimney appears as an interesting alternative since solar energy is a renewable and non-pollutant source of energy. These devices are capable of generating electric power through solar radiation. According to Maia *et al.* (2005a), a typical solar chimney consists on a tubular central tower, a solar collector, with a coverage made of a translucent material, and a turbine with a generator as can be seen in the Fig. 1. A part of the incident solar radiation is transmitted by the coverage and reaches the ground. The solar radiation absorbed by the soil increase its temperature, causing a convection heat transfer between the ground and the air under the cover. Therefore, the air mass inside the dispositive is heated and flows to the tower due to the buoyancy forces in function of the temperature gradients. This process happens during the insolation period. However, during the night, when there is no more solar radiation, a portion of the thermal energy stored in the deeper layers of the soil is transferred to the air, which allows the continuous operation of the system (Ferreira *et al*., 2006). The airflow generated by natural convection and chimney effect drives a wind turbine coupled to an electric generator (Yetimgeta and Mulugeta, 2014).

In 1981, the first solar chimney plant was built in Manzanares, Spain. This prototype had a tower with 195 m high and 10 m of diameter, with a coverage with 240 m of diameter and a height variable of 2 m in the entrance and 6 m in the center of the cover, generating 50kW of electrical power (Schlaich and Schiel, 2000). This device showed that large plants are necessary to generate energy with viable costs to be competitive with conventional power plants, because the efficiency of the conversion from solar to electric energy is low. Then, Ferreira *et al.* (2006) and Maia *et al.* (2005b) proposed a new application for smaller plants, where the hot airflow generated in the solar chimney can be used to dry agricultural products.

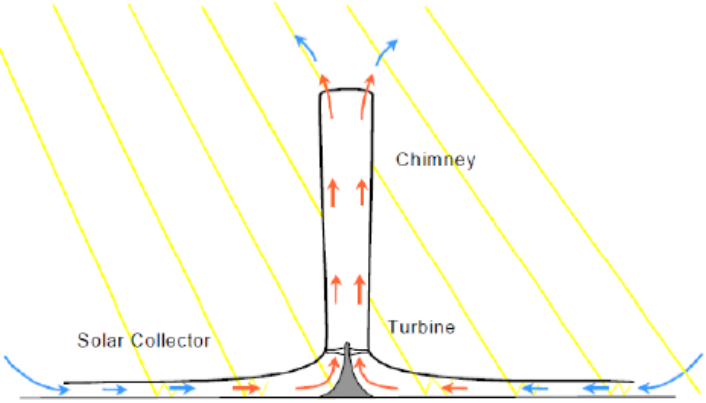

Figure 1: Schematic of a solar chimney (Schlaich and Schiel, 2000).

According to Ferreira *et al.* (2006), in order to evaluate the solar chimney as a radial solar dryer a prototype was built in the Federal University of Minas Gerais. The tubular tower was constructed in wood and covered in fiberglass, with the height of 12,3 m and the diameter of 1 m. A thermo-diffuser plastic film was used as translucent material for the circular coverage. The cover has a diameter of 25 m. The ground was built in concrete and painted in black color to increase the radiation absorption.

As previously explained, the ground plays an important function in the operation of the solar chimney, since the energy stored in its deeper layers allows the continuous operation of the system. According to Marinho Junior *et al.* (2015), an assessment of the ground directly affects the flow conditions in a numerical analysis. In this sense, the purpose of this paper is to evaluate the influence of the ground in the numerical analysis of the turbulent airflow in a small solar chimney as the prototype previously cited. Marinho Junior *et al.* (2015) did a numerical analysis of the turbulent airflow using the *k-ε* turbulence model, in addition this paper examines the analysis with the standard *k-ω* and the *SST k-ω* turbulence model.

2. MATHEMATICAL MODEL

The governing equations are given in cylindrical coordinates (r,x), so the conservation of mass, momentum (r,x) and energy written for average quantities are described respectively by:

$$\frac{\partial \rho}{\partial t}+\frac{\partial(\rho u)}{\partial x}+\frac{1}{r}\frac{\partial}{\partial r}(r\rho v)=0 \tag{1}$$

$$\frac{\partial(\rho u)}{\partial t}+\frac{\partial(\rho uu)}{\partial x}+\frac{1}{r}\frac{\partial}{\partial r}(r\rho uv)=-\frac{\partial}{\partial x}\left(p+\frac{2}{3}\rho k\right)+\frac{\partial}{\partial x}\left(\mu_e\frac{\partial u}{\partial x}\right)+\frac{1}{r}\frac{\partial}{\partial r}\left(r\mu_e\frac{\partial u}{\partial r}\right)+\frac{\partial}{\partial x}\left(\mu_e\frac{\partial u}{\partial x}\right)+\frac{1}{r}\frac{\partial}{\partial r}\left(r\mu_e\frac{\partial v}{\partial x}\right)+(\rho_0-\rho)g \tag{2}$$

$$\frac{\partial(\rho v)}{\partial t}+\frac{\partial(\rho uv)}{\partial x}+\frac{1}{r}\frac{\partial}{\partial r}(r\rho vv)=-\frac{\partial}{\partial r}\left(p+\frac{2}{3}\rho k\right)+\frac{\partial}{\partial x}\left(\mu_e\frac{\partial v}{\partial x}\right)+\frac{1}{r}\frac{\partial}{\partial r}\left(r\mu_e\frac{\partial v}{\partial r}\right)+\frac{\partial}{\partial x}\left(\mu_e\frac{\partial u}{\partial r}\right)+\frac{1}{r}\frac{\partial}{\partial r}\left(r\mu_e\frac{\partial v}{\partial r}\right)-2\mu_e\frac{v}{r^2} \tag{3}$$

$$\frac{\partial(\rho T)}{\partial t}+\frac{\partial(\rho uT)}{\partial x}+\frac{1}{r}\frac{\partial}{\partial r}(r\rho vT)=\frac{\partial}{\partial x}\left[\left(\frac{\mu}{\mathrm{Pr}}+\frac{\mu_t}{\mathrm{Pr}_t}\right)\frac{\partial T}{\partial x}\right]+\frac{1}{r}\frac{\partial}{\partial r}\left[r\left(\frac{\mu}{\mathrm{Pr}}+\frac{\mu_t}{\mathrm{Pr}_t}\right)\frac{\partial T}{\partial r}\right]+\frac{\beta T}{c_p}\left[\frac{\partial p}{\partial t}+\frac{\partial(pu)}{\partial x}+\frac{1}{r}\frac{\partial}{\partial r}(rpv)-p\frac{\partial u}{\partial x}-\frac{p}{r}\frac{\partial(rv)}{\partial r}\right] \tag{4}$$

The adopted models consider the two-dimensional turbulent flow in a steady state and the hypotheses for the solution are based on incompressible airflow, constant properties and Newtonian fluid. Where c_p, ρ, β and Pr are the air specific heat, density, volumetric expansion coefficient and Prandlt number. The subscript *"t"* indicates the turbulent amount. The effective viscosity μ_e, given as

$$\mu_e = \mu + \mu_t \tag{5}$$

Where μ is the viscosity of the air and μ_t is the viscosity of the flow or eddy viscosity. In this paper, the standard *k-ε*, standard *k-ω* and the *SST k-ω* turbulence model was used to compute the turbulent viscosity.

2.1 k-ε Standard Model

According to Stockinger (2016), the *k-ε* is a model of two differential equations, one for the turbulence kinetic energy, *k*, and another for rate of dissipation, *ε*, and the eddy viscosity is defined as:

$$\mu_t = \frac{\rho C_\mu k^2}{\varepsilon} \tag{6}$$

Where C_μ and ρ represent an empirical constant and density, respectively. The transport equations for *k* and *ε* are given by, respectively:

$$\frac{\partial(\rho k)}{\partial t} + \frac{\partial\left(\rho u_j k\right)}{\partial x_j} = \frac{\partial}{\partial x_j}\left[\left(\mu + \frac{\mu_t}{\sigma_k}\right)\frac{\partial k}{\partial x_j}\right] + G_k + G_b - \rho\varepsilon \tag{7}$$

$$\frac{\partial(\rho \varepsilon)}{\partial t} + \frac{\partial\left(\rho u_j \varepsilon\right)}{\partial x_j} = \frac{\partial}{\partial x_j}\left[\left(\mu + \frac{\mu_t}{\sigma_\varepsilon}\right)\frac{\partial \varepsilon}{\partial x_j}\right] + C_{1\varepsilon}\frac{\varepsilon}{k}(G_k + G_b) - C_{2\varepsilon}\rho\frac{\varepsilon^2}{k} \tag{8}$$

Where G_k is the generation of turbulence kinetic energy due to the mean velocity gradients, G_b the generation of turbulent kinetic energy due to fluctuations, $C_{1\varepsilon}$ and $C_{2\varepsilon}$ are constant, σ_k and σ_ε are the turbulent Prandtl number for *k* and *ε*.

Table 1 - Coefficients for the k-ε model.

Model	$C\mu$	$C_{1\varepsilon}$	$C_{1\varepsilon}$	σ_k	σ_ε
Standard k-e	0.09	1.44	1.92	1.0	1.3

2.2 k-ω Standard Model

According to Wilcox (2006), the standard model *k-ω* is an empirical model based on the transport of vorticity ($\omega = kl^{-2}$), which can also be considered as the specific dissipation rate, where *k* is the turbulent kinetic energy and *l* is a characteristic length. In this model of two partial differential transport equations, one for *k* and another for *ω*, the eddy viscosity is given by:

$$\mu_t = \alpha^* \frac{\rho k}{\omega} \tag{9}$$

The differential equations for *k* and *ω* are described respectively by:

$$\frac{\partial(\rho k)}{\partial t} + \frac{\partial\left(\rho u_j k\right)}{\partial x_j} = \frac{\partial}{\partial x_j}\left[\left(\mu + \frac{\mu_t}{\sigma_k}\right)\frac{\partial k}{\partial x_j}\right] + P_k - Y_k \tag{10}$$

$$\frac{\partial(\rho\omega)}{\partial t}+\frac{\partial\left(\rho u_j\omega\right)}{\partial x_j}=\frac{\partial}{\partial x_j}\left[\left(\mu+\frac{\mu_t}{\sigma_\omega}\right)\frac{\partial\omega}{\partial x_j}\right]+G_\omega-Y_\omega \tag{11}$$

where σ_k=2.0 and σ_ω=2.0 are the turbulent Prandtl number of k and ω. The coefficient α^* dampens the turbulent viscosity, resulting in a correction for the low Reynolds number. P_k and G_ω are production terms, Y_k and Y_ω are destruction terms of each quantity.

2.3 SST k-ω Model

This model was developed for aeronautical flows simulations with strong adverse pressure gradients with the best behavior of the κ–ε and κ–ω models. For boundary layers flows, the κ–ω model is superior to the k-ε model in the solution of the viscous near-wall region, and has been successful in problems with adverse pressure gradients. However, the κ–ω model requires a non-zero boundary condition on ω for non-turbulent free stream, and the calculated flow is very sensitive to the value specified and the κ-ε model does not suffer this deficiency (Menter, 1992).

Therefore, the *SST* model combine the robust and precise formulation of the κ–ω model close to walls with the free stream independence of the κ–ε model outside the boundary layer. To get this, the κ–ε model is written in terms of ω. Then the standard κ–ω model and the transformed κ–ε model are both multiplied by a blending function and both models are added together. This mixing function F_1 is one (conducting to the standard κ–ω model) at the inner edge of a turbulent boundary layer and changes to zero (corresponding to the standard κ–ε model) at the outer edge of the layer. According to Menter *et al.* (2003), the turbulent kinetic energy κ and specific dissipation rate ω of the *SST* model is given by:

$$\frac{\partial k}{\partial t}+u_j\frac{\partial k}{\partial x_j}=\frac{\partial}{\partial x_j}\left[\left(\upsilon+\sigma_k\upsilon_t\right)\frac{\partial k}{\partial x_j}\right]+P_k-\beta^*K\omega \tag{12}$$

$$\frac{\partial\omega}{\partial t}+u_j\frac{\partial\omega}{\partial x_j}=\frac{\partial}{\partial x_j}\left[\left(\upsilon+\sigma_\omega\upsilon_t\right)\frac{\partial\omega}{\partial x_j}\right]+\alpha S^2-\beta\omega^2+2(1-F_1)\sigma_{\omega2}\frac{1}{\omega}\frac{\partial k}{\partial x_i}\frac{\partial\omega}{\partial x_i} \tag{13}$$

The kinematic eddy viscosity is given by:

$$\upsilon_t=\frac{\alpha_1 k}{\max(\alpha_1\omega,SF_2)} \tag{14}$$

Auxiliary relations are given below:

$$F_1=\tanh\left[\left[\min\left[\max\left(\frac{k^{1/2}}{\beta^*\omega y},\frac{500\upsilon}{y^2\omega}\right),\frac{4\sigma_{\omega2}k}{CD_{k\omega}y^2}\right]\right]^4\right] \tag{15}$$

$$F_2=\tanh\left[\left[\max\left(\frac{2k^{1/2}}{\beta^*\omega y},\frac{500\upsilon}{y^2\omega}\right)\right]^2\right] \tag{16}$$

$$P_k=\min\left[\upsilon_t S^2;10\beta^*k\omega\right] \tag{17}$$

$$CD_{k\omega}=\max\left(2\rho\sigma_d\frac{1}{\omega}\frac{\partial k}{\partial x_i}\frac{\partial\omega}{\partial x_i},10^{-10}\right) \tag{18}$$

$$\phi=\phi_1F_1+\phi_2(1-F_1) \tag{19}$$

According to Miranda and Rezende (2013), ϕ represent the set of closure constants for the *SST* model and ϕ_1 and ϕ_2 represent the constants from the standard *k-ω* and *k-ε* models, respectively. The constants ϕ are calculated using a blend between the constants ϕ_1 (*k-ω*) and ϕ_2 (*k-ε*), which can be seen in Tab. 2, as:

Table 2. Closure coefficients of the SST model.

	β	$\beta*$	σ_κ	σ_ω	σ_d	α
ϕ_1 (standard κ–ω)	0.075	0.09	0.5	0.5	0.856	5/9
ϕ_2 (standard κ–ε)	0.0828	0.09	1.0	0.856	0.856	0.44

3. NUMERICAL METHODOLOGY

The numerical analysis of the turbulent airflow in a small solar chimney used in this paper was based in the work of Marinho Junior *et al.* (2015). The tower of solar chimney has 12.3 m high and 1 m in diameter, the collector has 25 m of diameter and variable height relative to the ground. Using the concept of axisymmetric, the dimensions of the chimney can be seen in the Fig. 2.

To solve the governing equations, the software ANSYS-FLUENT 15.0 was used, in which the discretization was based on the Finite Volume Method, the Multigrid iterative method was used to solve the system of algebraic equations and the pressure and velocity were coupled using SIMPLE algorithm scheme (Patankar and Spalding, 1972).

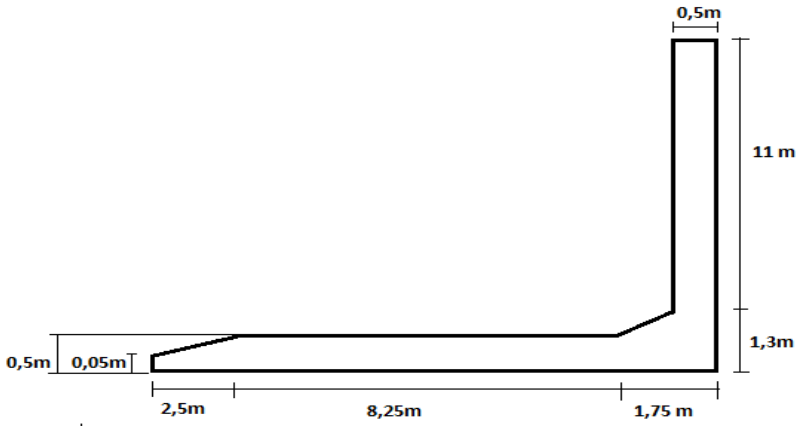

Figure 2: The geometric dimensions of the solar chimney.

The boundary conditions adopted are showed in the Figure 3 and they are based in the work of Marinho Junior *et al.* (2015).

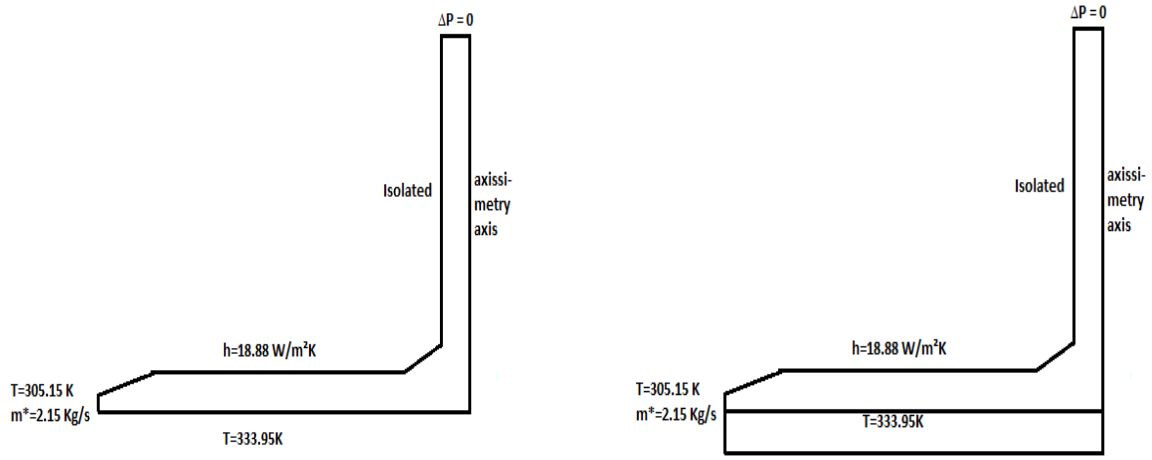

Figure 3: Boundary conditions for numerical analysis.

For boundary conditions, prescribed temperature of 333.95 K was used for the ground, the tower was assumed adiabatic and the coefficient of heat exchange by convection for the coverage was equal to 18.88 W/m²K. The conditions for the air at inlet is ambient temperature (305.15 K) with a mass flow of 2.15 kg/s (Marinho Junior *et al.*, 2015). The tower walls, the ground, the coverage and the junction between the cover and the tower are all wall regions and the non-slip conditions were assumed.

The purpose in the work is to evaluate the influence of the ground as an energy storage layer in the numerical analysis, therefore two simulations were made, first the geometry was defined as the coverage and the tower, assuming that the ground is a constant surface. The second assuming the ground under the surface with a depth of 0.5 m. This last choice was based in the work of Maia *et al.* (2005b), in which they showed that the ground under the surface was covered with a 0,5 m concrete layer, painted black to increase the solar radiation absorbed and that the differences of temperature along the time are insignificant for depths superior to 0.4 m.

4. RESULTS

As discussed in this work, the energy stored by the ground is extremely important for the continuous operation of the solar chimney. Because during the day the solar energy is transferred to the deeper soil layers and then at night when there is no more incidence of solar radiation, the heat flux is reversed and the heat stored in the soil is transferred to the ground surface. Consequently, the airflow in the solar chimney continues unceasingly along the day.

The results below are referents two simulations cited previously. They were performed using the *k-ε*, *k-ω* and standard *SST k-ω* turbulence models. Also is showed the results obtained from Marinho Jr. *et al*. (2015), who used the *k-ε* model. From the results, the influence of the energy storage layer in the numerical simulation is evaluated.

The air entering in the solar chimney follows in the radial direction of the collector and on the junction between the collector and the tower there is a change in the air flow to the the axial direction of the tower. Due to the reduction of area in this position, the velocity increases in the tower and only small variations in the velocity profile are observed, however the average velocity remains constant, since the diameter does not change in the tower.

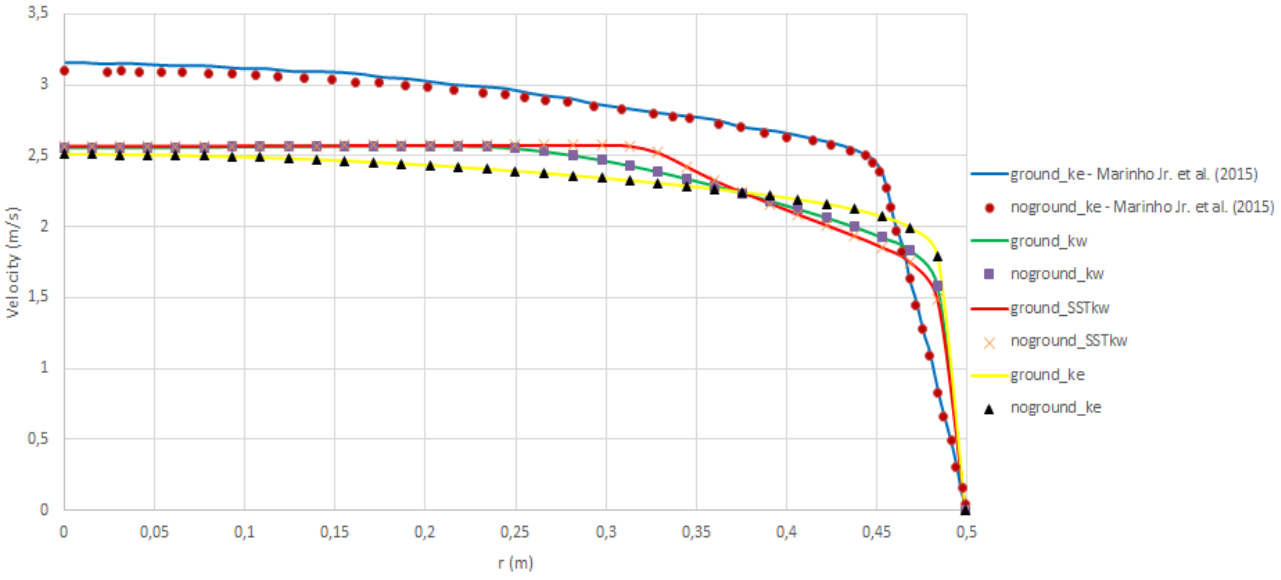

Figure 4. Velocity profile in the tower.

The Figure 4 shows the velocity profile in the tower, evaluated at a position corresponding to half the tower height. From the graphic, it is possible to observe the variation of the velocity with the radius of the solar chimney. For all turbulence models used in the numerical simulation, the velocity is maximum in the center of the chimney (r=0) and as it approaches the wall the velocity tends to zero due to the non-slip condition. According to Maia *et al.* (2005a), in the period of highest temperature during the day, the air velocity experimental in the tower was 2.2 m/s. Then, the numerical simulation for three different models seen in this paper presented great results, since the average velocity in the tower was around 2.3 m/s. The velocity profiles obtained in all turbulence models are typical of turbulent flow, as expected. Considering the numerical simulation with and without the ground, small variations are observed being negligible. This has occurred in numerical simulations for all models, including the simulation of Marinho Jr. *et al.* (2015). The figures below show the temperature fields along the solar chimney for the models *k-ε*, *k-ω* and *SST k-ω*, for the geometry without and with the ground, respectively.

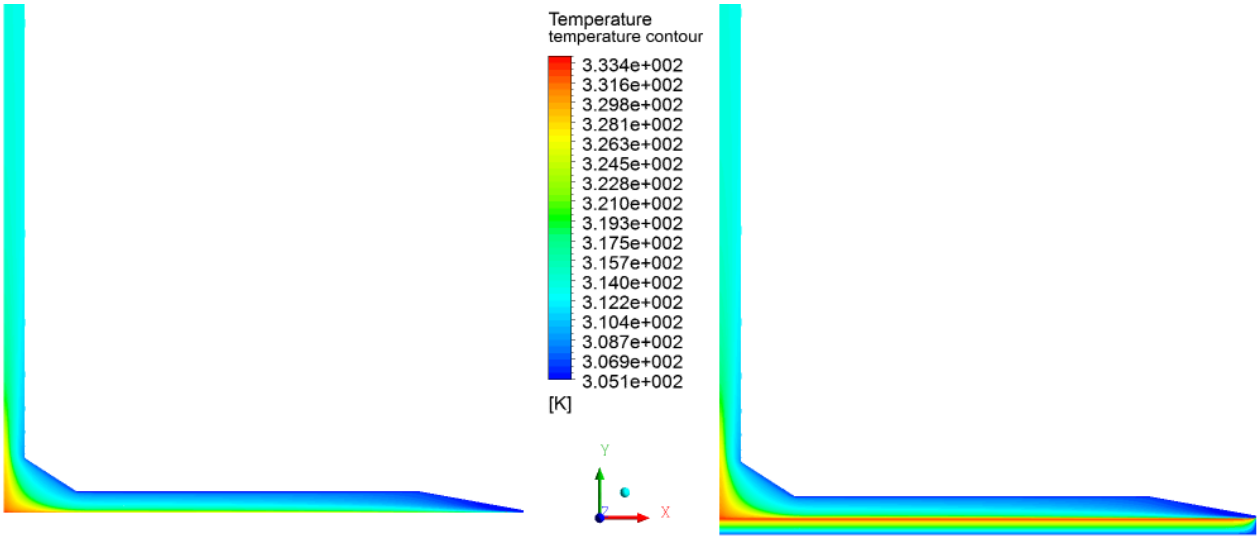

Figure 5. Temperature profile in the solar chimney in the numerical simulation using the standard $k\varepsilon$ model.

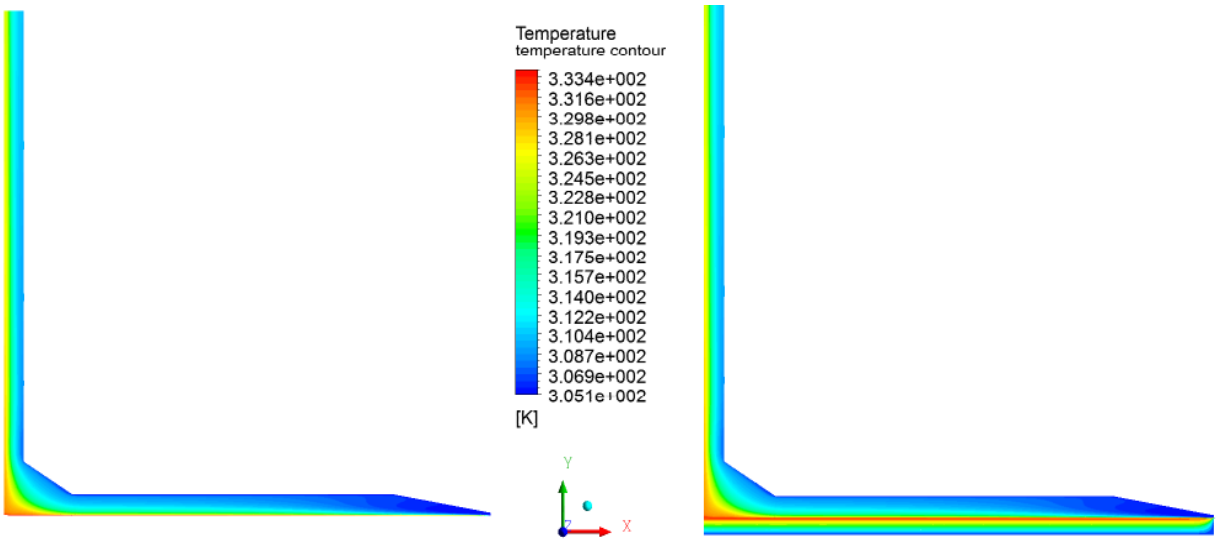

Figure 6. Temperature profile in the solar chimney in the numerical simulation using the standard $k\omega$ model.

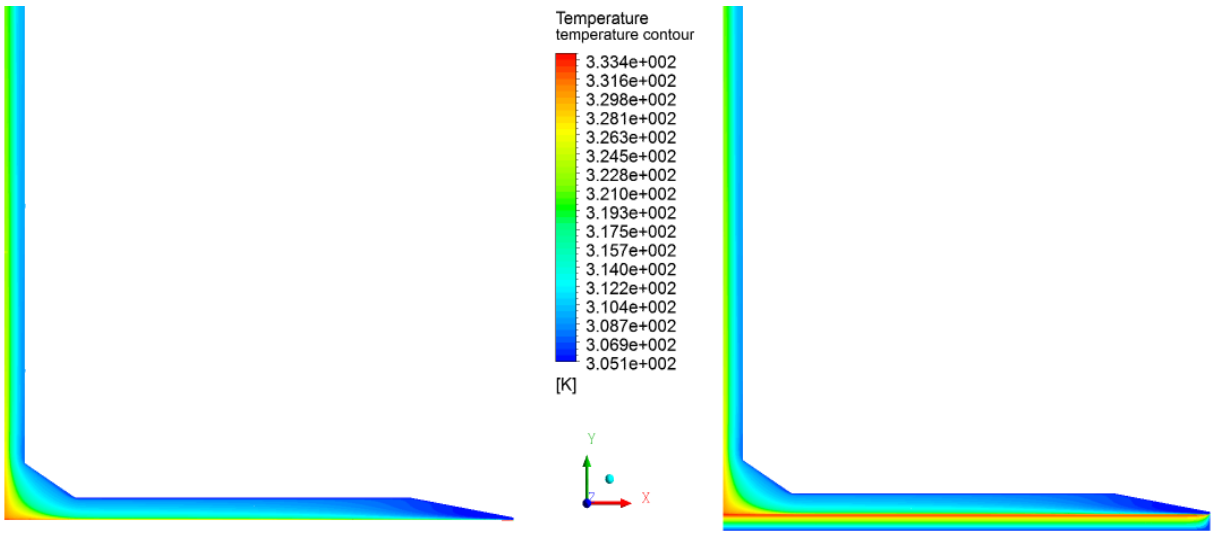

Figure 7. Temperature profile in the solar chimney in the numerical simulation using the *SST-kω* model.

The influence of the ground as an energy storage layer did not lead to significant changes in temperatures distribution along the solar chimney, when comparing the same turbulence model, as shown in Figures 5, 6 and 7. That is, the numerical simulation considering the ground as a solid, presented similar results with the simulation considering the ground with a constant surface. Despite the important role that the ground plays in the solar chimney, the heat transfer by conduction to the deeper layers does not significantly alter the thermal exchange between the air and the ground surface in the numerical analysis.

It was observed that the temperature distribution throughout the solar chimney was very similar for numerical simulation using the *k-ω* and *SST k-ω* models. In the numerical simulation using the *k-ε* model, a difference in the temperature distribution in the tower was seen in relation to the other two models. Such differences will be discussed in the analysis of Figure 9.

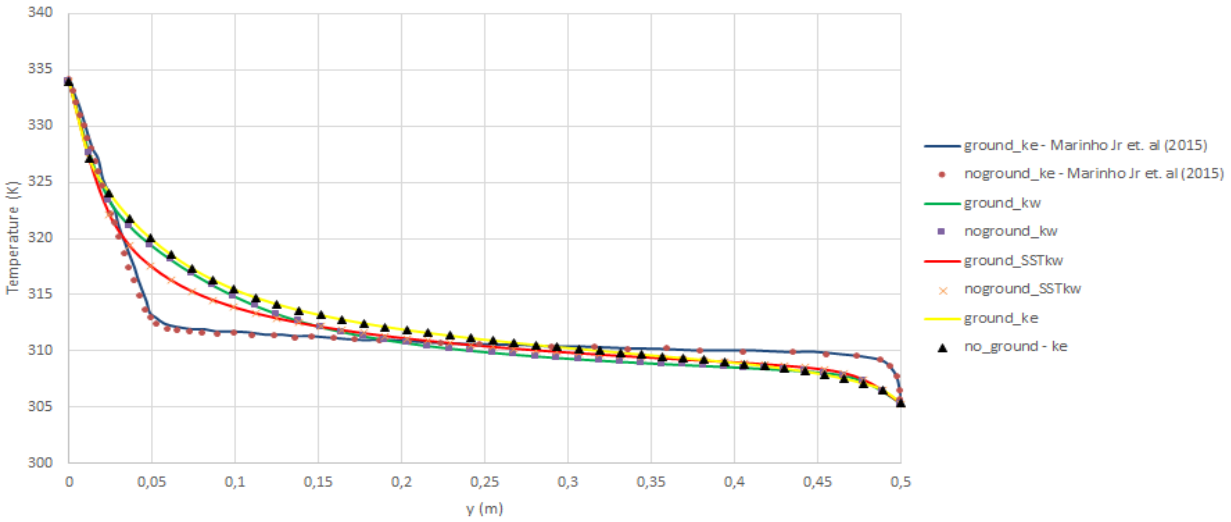

Figure 8. Temperature profile in the coverage.

The Figure 8 shows the temperature profile in the coverage, in an axial position corresponding to half the coverage radius. From the graphic, it is possible to observe the variation of the temperature with the collector height. For all turbulence models used in the numerical simulations, the temperature is highest in the regions close to the ground surface (y=0) and tend to free stream temperature in the surface the cover (y=0.5 m). The three turbulence models used in the numerical simulation presented good agreement for the temperature along the collector height, mainly for the central region. According to Maia et al. (2005a), in the period of highest temperature along the day, the temperature experimental in y=0,25 m was around 310 K. Then, the numerical simulation for three different models seen in this paper presented satisfactory results for the temperature in the coverage. As it was already observed in the temperature fields, for the same turbulence model, the numerical simulation with and without the ground presented identical results for temperature in the coverage, including the simulation of Marinho Jr. *et al.* (2015).

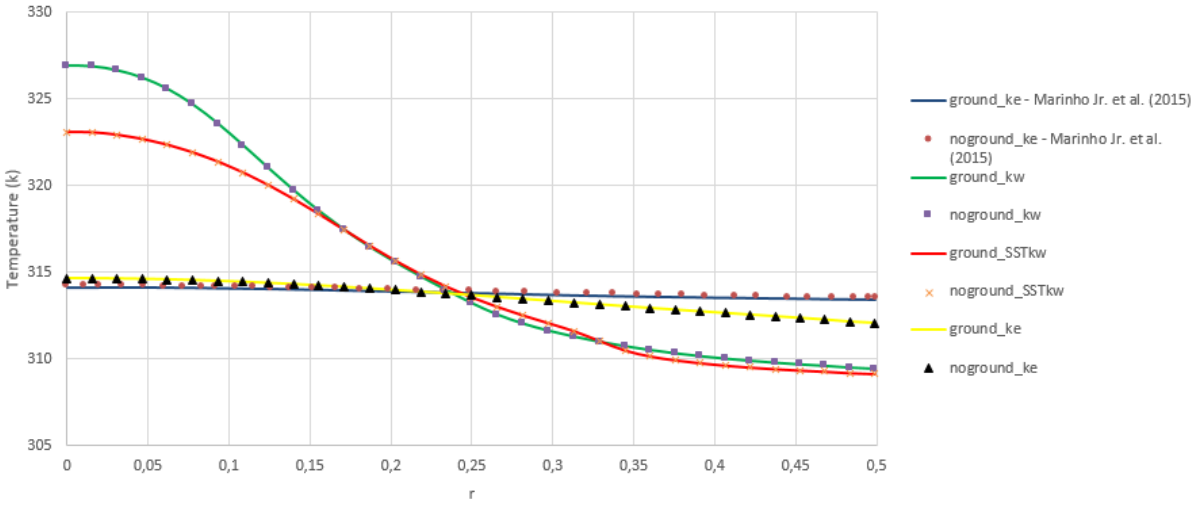

Figure 9. Temperature profile in the tower.

Figure 9 shows the temperature profile in the tower, evaluated at a position corresponding to half the tower height. From the graphic, it is possible to observe the variation of the temperature with the radius of the solar chimney. As was seen previously in the temperature fields, in the central region of the tower, the numerical simulation using the *k-ε* turbulence model presented differences in relation to the numerical simulation using the *k-ω* and *SST k-ω*. For all turbulence models, the numerical simulation showed that the temperature in the center is larger and decreases toward the tower wall. In the numerical simulation of this work with the *k-ε*, as in the simulation done by Marinho *et al*. (2015) using the same turbulence model, it is perceived that this decrease is small and the temperature does not change much in the radial direction of the tower. For both, the average temperature in the cross section is around 313 K and the airflow is approximately isothermal.

This situation was not observed for the numerical simulations using the *k-ω* and *SST k-ω* turbulence models, since in these simulations larger temperature variation between the center and the tower wall was seen. The air that is nearest to the ground has a higher temperature, since the ground surface has a prescribed temperature of 333.95 K (boundary condition), and as the collector height increases this temperature decreases, as discussed in Figure 8. At the junction between the solar collector and the tower, there is a change in the flow direction, then the air that was in the collector upper layers with a lower temperature tends to go to the nearest part of the tower wall. Moreover, the air that is closer to the ground, with a higher temperature tends to go to the central region, therefore higher temperatures are observed in this position. Evidently, the air flow is turbulent and the tower is considered adiabatic, so at a certain chimney height the fluid temperature redistributes inside the tower and the isothermal flow behavior is reached, since the heat can not escape through the boundaries.

In addition, the experimental data of Maia *et al.* (2015b) showed that for a same height in the tower, the temperature does not present larger variations in the radial direction, therefore for the thermal analysis in the tower region, the *k-ε* turbulence model showed a better behavior. For positions from r=0,25 m up to the tower wall, the temperature values in the tower approximate among all the simulated models. The main objective in this work is to evaluate the influence of the ground in the numerical analysis and, again, can be observed that, for the same turbulence model, the numerical simulation with and without the ground presented identical results, including the simulation of Marinho Jr. *et al*. (2015).

5. CONCLUSION

Growing energy consumption and concerns about climate change have encouraged the search for cleaner and more reliable energies. Inside this context, solar chimney is a good alternative. Airflow numerical simulations in this device appear as a great alternative for engineers to evaluate the thermal and dynamic conditions of the flow, and consequently to evaluate the technical and economic viability of the plant.

The results showed that despite the important behavior that the ground performs in the continuous operation of the solar chimney, the use of the ground as energy storage layer in the numerical analysis can be neglected, since the simulation considering the ground as a solid presented similar results with the simulation considering the ground as a constant surface.

The results showed that the k-ε turbulence model represented better the thermal analysis in the tower, since the experimental data showed that in this region the temperature does not change much in the radial direction. For the other regions in the solar chimney, all models presented results with good agreement.

Evidently, the analysis done in this work is valid for the prototype with geometric dimensions and boundary conditions established, if some of these parameters change, differences may be observed.

6. ACKNOWLEDGEMENTS

The authors are grateful to CAPES for the financial support receiving during the realization of this work.

7. REFERENCES

Ferreira, A.G.; Maia, C.B.; Valle, R.M.; Cortez, M.F.B. 2006. “Balanço energético de uma chaminé solar”. In Proceedings of the RECIE 2006, RECIE2006, Uberlândia, Brazil.

Maia, C.B.; Ferreira, A.G.; Valle, R.M; Cortez, M.F.B. 2005a. “Experimental and Theoretical Evaluation of a Solar Chimney test plant part I: Theoretical Treatment” In Proceedings of the COBEM 2005, Ouro Preto, MG, Brazil.

Maia, C.B.; Ferreira, A.G.; Valle, R.M; Cortez, M.F.B. 2005b. “Experimental and Theoretical Evaluation of a Solar Chimney test plant part II: Experimental results” In Proceedings of the COBEM 2005, Ouro Preto, MG, Brazil.

Marinho Junior, P. F.; Fernandes, T.S.; Castro Silva, J. O.; Hanriot, S. M.; Maia, C. B. 2015. “Evaluation of the Boundary Conditions for the Ground in the Numerical Analysis of a Solar Chimney”, COBEM2015, Rio de Janeiro, RJ, Brazil.

Menter, F. R., 1992. “Influence of Free Stream Values on *k-ω* Turbulence Model Predictions”, AIAA Journal, Vol. 30, No. 6, pp. 1657-1659.

Menter, F. R.; Kuntz, M.; Langtry, R. 2003. “Ten Years of Industrial Experience with the SST Turbulence Model”, Proceedings of the 4th International Symposium on Turbulence, Heat and Mass Transfer, pp. 625-632.

Miranda, W. R. and Rezende, A. L. T. 2013. “Rans Models Apllied in a Flow Over a Rounded Edge”, 22nd International Congress of Mechanical Engineering (COBEM 2013), Ribeirão Preto, SP, Brazil.

Patankar, S. V. and Spalding D. B. 1972. “A calculation procedure for heat, mass and momentum transfer in three-dimensional parabolic flows”. International Journal of Heat and Mass Transfer, Vol. 15, pp. 1787-1806.

Schlaich, J. and Schiel, W. 2000. Solar Chimneys – Encyclopedia of Physical Science and Technology. Schlaich Bergermann und Partner, Stuttgart, 3nd edition.

Stockinger, C. A. 2016. Numerical Analysis of Airflow and Output of Solar Chimney Power Plants. Master of Science in Mechanical Engineering. Blacksburg, V.A.

Wilcox, D. C. 2006. Turbulence Modeling for CFD, 3rd edition, DCW Industries, Inc., La Canada CA, 2006.

Yetimgeta, B. and Mulugeta, N. 2014. Modeling and Simulation of Solar chimney Power Plant for Electrification: Dire Dawa. International Journal of Research in Mechanical Engineering.

8. RESPONSIBILITY NOTICE

The authors are the only responsible for the printed material included in this paper.